A PPM-based Flux Form Semi-Lagrangian Model for Regional Weather and Climate Predictions. Part I: The Unified Shallow Water Model

Shian-Jiann Lin
Data Assimilation Office, Laboratory for Atmospheres, GSFC/NASA, MD, 20771, USA
and
Tzay-Ming Leou
Computer Center, Central Weather Bureau, Taiwan, ROC

Abstract

A unified shallow water model based on the Flux Form Semi-Lagrangian (FFSL) scheme is described. This is a unified model in the sense that it can be used as a global model, a regional model, or a fully interactive multiply nested global-regional model. A novel two-grid system: the "inverse Z grid", which has the advantage of Randall's Z grid but without the need to invert vorticity and divergence, is developed. The nesting capability of the model is first tested by verifying the predictions from the nested model against that from the global model at the same fine grid resolution. The evolution of Typhoon-like vortex is simulated using the fully interactive triply nested global-regional mode of the unified model. Owing to the upwind-biased nature of the FFSL scheme and the application of the monotonicity constraint, no explicit damping mechanism of any kind is needed, even when the model in run in the multiply nested global-regional mode. The vortex can enter and leave the boundary of the local fine grid domain without generating noises commonly found in nested grid models.

1. Introduction

Arakawa-type finite difference method (Arakawa and Lamb 1981) and the spectral method (e.g., Bourke 1972), at least in the 80's, are the two most dominant modeling techniques for Numerical Weather Predictions (NWP) and climate simulations. As computer power rapidly increases in the past decade, so is the demand for a higher level of predictability. Deficiencies in the above two modeling methods are becoming more apparent. Arakawa-type finite differencing methods suffer from the so-called "pole-Courant number problem", which not only limits the size of the largest time step but also introduces computational noises near the poles, which is made worse by the existence of the so-called "Hollingsworth-Kållberg instability" (Hollingsworth et al. 1983). The spectral method formally has no pole problem but its computational efficiency decreases rapidly as the resolution increases (due to the "slow" Legendre transform). Furthermore, it is difficult to apply the spectral method to a limited area and/or using the *domain decomposition technique* on a massively parallel platform. These and other problems have motivated the recent rapid development of the semi-implicit semi-Lagrangian method (see Staniforth and Côté 1991 for a review).

Traditional semi-Lagrangian method (SLM) has several deficiencies as well. The most notable and perhaps most serious problem is that mass is not conserved due to the fact that the non-conservative advective form of the equations are solved. The non-conservation problem can lead to serious systematic biases in long term integrations. Another problem, which is not unique to the SLM*, is that it is not free of the numerical over- and under-shoots (i.e., Gibbs oscillations). An obvious consequence of this problem is that the predicted mixing ratios of water substances can become unphysically negative. Although less obvious, similar over- and under-shoots also exist in the predicted temperature and the wind fields. Moreover, problems in the model that are induced by the Gibbs oscillations can be mistakenly identified as deficiencies in the model's physics. This type of numerical problem often leads to incorrect compensating tuning of the true physics. In addition, a very strong and *ad hoc* numerical diffusion is often required near the lateral boundaries of a nested grid regional model.

The numerical method adopted here is based on the recently developed multi-dimensional Flux-form semi-Lagrangian (FFSL) transport scheme of Lin and Rood (1995a, LR-a hereafter). The strictly 1-D Piecewise Parabolic Method (PPM, Colella and Woodward 1984) is used as the basic building block of the mass-conserving multi-dimensional FFSL scheme. The monotonicity constraint used in the PPM can be regarded as a built-in subgrid scale parameterization in the sense that no explicit numerical diffusion is needed to obtain a noise free high-resolution solution. In the original PPM formulation, a complicated Riemann solver is required when the full hydrodynamic equation set is solved. The

* Williamson and Rasch (1989) developed 2-D shape-preserving semi-Lagrangian interpolation schemes that are free of the under- and over-shoots problem, at the expense of somewhat larger computational damping.

Riemann solver is devised principally for the transonic or supersonic flows involving shock waves, which are the rule rather than the exception in aerodynamic or astrophysical applications (e.g., Woodward and Colella 1984). Geophysical flows, on the other hand, are dominated by smoothly varying large-scale waves, which is particularly true from a global perspective (e.g., in climate simulations or medium range weather forecasts). Our objective here is to apply the FFSL scheme, a multi-dimensional transport scheme initially developed for passive scalars, to model geophysical flows in an accurate and computationally efficient manner. To this end, we shall apply a more conventional approach for computing the pressure gradient terms and the "time-averaged advective winds" (see Lin and Rood 1995b for details, LR-b hereafter) in lieu of solving a very difficult and time consuming multidimensional Riemann problem. As to be described in the next section, for the shallow water system of equations, the FFSL transport scheme will be applied directly to the conservation law for the "mass" and indirectly to the conservation law for the "absolute vorticity" using the "inverse Z grid" (a combination of the C and the D grid, see Fig. 1), which has the advantage of the Z grid (Randall 1994) but without the need to invert vorticity and divergence, a tremendous computational advantage.

To facilitate the construction of a flexible unified model that can be used as a global model, a regional model, or a nested global-regional model, the discretization of the governing equations should be strictly local. A semi-implicit treatment of the gravity waves, which requires the solution of an elliptic equation, should therefore be avoided. The economical explicit "forward-backward" scheme described by Mesinger and Arakawa (1976) for integrating the pressure gradient terms is stable and second order accurate when combined with a forward-in-time advection scheme. The FFSL scheme, a forward-in-time local discretization technique, is perfectly suited for this purpose. A very important advantage of the unified model approach is that full compatibility between the time dependent lateral boundary conditions (provided by a coarse grid model) and the fine grid regional model can be easily achieved. This is demonstrated by the numerical example described in section 4. We will first review the 2-D FFSL scheme in section 2. The discretization of the shallow water equations using the spherical coordinates is described in section 3. The specification of the boundary conditions, the nesting strategy, and a numerical example are given in section 4. Concluding remarks and related future works are given in section 5.

2. The 2-D FFSL scheme — a brief review

Central to the algorithm to be described in the next section is the FFSL transport scheme developed in LR-a. For brevity, only the fundamental aspect of the 2-D FFSL scheme will be given here. The conservation law for a density-like field Q (in the context of the shallow water equations, Q may represent the depth of the fluid h or the absolute vorticity Ω) is

$$\frac{\partial}{\partial t} Q \;+\; \nabla\cdot(\mathbf{V}\,Q) \;=\; 0 \tag{2.1}$$

where $\mathbf{V} = (u, v)$ is the horizontal vector velocity. To model Eq. 2.1 using 1-D finite-volume schemes (such as the PPM), we define F and G as the 1-D flux-form operators for updating Q for one time step in the longitudinal (λ) and latitudinal (θ) direction, respectively. Adopting the following standard notations for the *difference* and *average* operations,

$$\delta_\sigma q \;=\; q\left(\sigma+\frac{\Delta\sigma}{2}\right) \;-\; q\left(\sigma-\frac{\Delta\sigma}{2}\right) \tag{2.2}$$

$$\overline{q}^{\sigma} \;=\; \frac{1}{2}\left[q\left(\sigma+\frac{\Delta\sigma}{2}\right) \;+\; q\left(\sigma-\frac{\Delta\sigma}{2}\right)\right] \tag{2.3}$$

F and G can be written as follows.

$$F\left(u^{*}, \Delta t; Q^{n}\right) \;=\; -\frac{\Delta t}{A\Delta\lambda\cos\theta}\;\delta_\lambda\left[X\left(u^{*}, \Delta t; Q^{n}\right)\right] \tag{2.4}$$

$$G\left(v^{*}, \Delta t; Q^{n}\right) \;=\; -\frac{\Delta t}{A\Delta\theta\cos\theta}\;\delta_\theta\left[\cos\theta\, Y\left(v^{*}, \Delta t; Q^{n}\right)\right] \tag{2.5}$$

where A is the radius of the earth. X and Y, the "time-averaged fluxes" of Q in the longitudinal and latitudinal direction, respectively, are defined analytically as

$$X\left(u^{*}, \Delta t; Q^{n}\right) \;=\; \frac{1}{\Delta t}\int_{t}^{t+\Delta t} uQ\;dt \tag{2.6}$$

$$Y(v^*, \Delta t; Q^n) = \frac{1}{\Delta t} \int_t^{t+\Delta t} vQ \, dt \tag{2.7}$$

As illustrated in Fig. 1, the advective winds (u^*, v^*) and the Q field (h or Ω) are staggered as in the C-grid. For convenience, we will drop, for now, the dependence of the F and G operators on (u^*, v^*) and Δt. To derive the multidimensional FFSL scheme, the first step is to remove directional biases by averaging two anti-symmetric operator-split schemes. The resulting directional bias free scheme is

$$Q^{n+1} = Q^n + F[Q^n + \tfrac{1}{2}G(Q^n)] + G[Q^n + \tfrac{1}{2}F(Q^n)] \tag{2.8}$$

Scheme (2.8) still suffers from the "deformational error" (Smolarkiewicz 1982). An immediate consequence of this error is that a constant Q field will not remain constant when the flow is non-divergent. To remove this error, the second step is to replace F and G inside the square brackets in (2.8), the contributions from the cross-stream directions, with their *advective-form* counter part f and g, respectively, to obtain the following form of the 2-D FFSL scheme.

$$Q^{n+1} = Q^n + F[Q^n + \tfrac{1}{2}g(v_a^*, \Delta t; Q^n)] + G[Q^n + \tfrac{1}{2}f(u_a^*, \Delta t; Q^n)] \tag{2.9}$$

where $u_a^* = \overline{u^*}^{\lambda}$, $v_a^* = \overline{v^*}^{\theta}$. The generalization of scheme 2.9 to large time step (Courant number greater than one), which only involves slight modification to the 1-D operators, is described in LR-a.

3. Discretization of the shallow water equations using the 2-D FFSL scheme

The mass conservation law for a shallow layer of "water" is

$$\frac{\partial}{\partial t} h + \nabla \cdot (\mathbf{V} h) = 0 \tag{3.1}$$

where h represents the depth of the fluid (the "mass" in the shallow water system). The vector invariant form of the momentum equation in the spherical coordinates can be written concisely in component form as follows.

$$\frac{\partial}{\partial t} u = \Omega v - \frac{1}{A \cos\theta} \frac{\partial}{\partial \lambda} [\kappa + \Phi] \tag{3.2}$$

$$\frac{\partial}{\partial t} v = -\Omega u - \frac{1}{A} \frac{\partial}{\partial \theta} [\kappa + \Phi], \tag{3.3}$$

where

$\Phi = \Phi_s + gh$, the free surface geopotential (g is the gravitational acceleration),

Φ_s = the surface geopotential,

$\Omega = 2\omega \sin\theta + \nabla \times \mathbf{V}$, the absolute vorticity,

ω = angular velocity of the earth,

$\kappa = \frac{1}{2}\mathbf{V} \cdot \mathbf{V}$, the kinetic energy.

A significant advantage of this form of the momentum equation is that the metric terms, which are singular at the poles, are absorbed into the definition of the relative vorticity, which is well defined (i.e., non-singular) at the poles. A disadvantage of this form is that the numerical form of the kinetic energy κ needs to be carefully formulated to minimize inconsistency between $\nabla\kappa$ and the absolute vorticity fluxes. This inconsistency manifests itself as a spurious momentum source and could result in what is called "Hollingsworth-Kållberg instability" (Hollingsworth et al. 1983).

The conservation law for the absolute vorticity can be readily obtained by taking curl of the vector momentum equation [i.e., $\nabla \times$ (3.2, 3.3)]

$$\frac{\partial}{\partial t}\Omega + \nabla\cdot(\mathbf{V}\,\Omega) = 0. \tag{3.4}$$

The divergence ($\eta=\nabla\cdot\mathbf{V}$) equation is obtained by applying the divergence operator to the same vector equation. If the vorticity-divergence form is chosen, a way must be found to invert the pair (Ω, η) back to (u, v) each time step for the time integration to proceed. The spectral transform method is ideally suited for this purpose because the inversion is nearly trivial. Due to the continuous differentiability of the basis functions used in the spectral transform method, there is no theoretical advantage for the spectral method to choose the vorticity-divergence form over the usual or the vector-invariant form of the momentum equations described above. There is, however, advantage for choosing the vorticity-divergence form when local discretization methods are used (The "Z grid", Randall 1994). Part of the advantage can be explained by the fact that the transport of the (absolute or relative) vorticity, a higher order conservative scalar, is being modeled directly. To retain this advantage while avoid inverting an elliptic equation, the idea introduced by Sadourny (1975) and Arakawa and Lamb (1981, AL hereafter) can be applied to discretize the vector-invariant form of the momentum equations. AL's method amounts to a subtle second order center-in-space discretization to (3.1), (3.2), and (3.3). Some design constraints are enforced to ensure that, after taking curl of the center differenced form of (3.2) and (3.3), the resulting vorticity equation is reduced to the celebrated "Arakawa Jocobian" for vorticity advection (Arakawa 1966) when the flow is non-divergent. The approach proposed here in some ways mirrors that of AL's, but in other ways is a complete opposite to their approach. The fundamental departures from their approach are outlined next.

The first and the most important difference is in the transport scheme itself and in the way absolute vorticity is transported in a more general divergent flow. AL's method is a center-differenced scheme and therefore it is possible to conserve both the total energy and potential enstrophy, in the point-wise sense. A subgrid scale mixing parameterization is generally required for realistic flows. In our approach, we seek to build the subgrid mixing process into the grid-scale transport process by using a physically motivated upstream-biased monotonicity-preserving finite-volume scheme — the multidimensional FFSL scheme developed in LR-a. It is applied explicitly to the transport of the fluid depth h and implicitly to the absolute vorticity Ω. The discretized h and Ω are considered as cell-averaged values, not point-wise values. Because the implied subgrid distribution is forced to be monotonic, no additional damping (subgrid scale mixing) mechanism is needed. The same scheme is used for transporting h and Ω, regardless of the divergence of the flow. Functional relations between h and Ω can therefore be better preserved. In AL's approach, the equation for the fluid depth (Eq. 3.1) is center differenced in a straightforward manner while (3.2) and (3.3) are center differenced, in a more sophisticated way, to achieve the goal of vorticity transport by the Arakawa Jacobian for nondivergent flow. Therefore, the transport scheme for h and Ω in AL's approach will be, in general, different. As a consequence, initial functional relationship between these two variables will be lost during the course of time integration. It is our view that the lost of the functional relation will have some negative impacts on the predictability of the flow.

To achieve the goal of transporting h and Ω in exactly the same manner, a basic requirement is that they be defined at the same point. Since our prognostic variables are h and (u, v), instead of h and (Ω, η), the D-grid arrangement (see Fig. 1) is the best choice. It is known that any grid, other than the C grid or the Z grid (Randall 1994), generates two-grid-interval gravity wave noises. We avoided this problem by computing the time-centered advective winds (u^*, v^*) directly on the C grid. We shall consider (u^*, v^*) as given and defer the discussion on how they are computed after the discretization of the governing equations on the D grid are presented.

It is observed that if the first term on the right hand side (r.h.s.) of 3.2 and 3.3, at the numerical level, is interpreted as the time-averaged latitudinal and longitudinal flux of the absolute vorticity, respectively, a consistently discretized absolute vorticity equation can be formed by taking curl, numerically, of these two discretized component equations. Directly from Eq. (2.9), the discretized transport equation for h and Ω are simply as follows.

$$h^{n+1} = h^n + F(u^*, \Delta t; h^\theta) + G(v^*, \Delta t; h^\lambda) \tag{3.5}$$

$$\Omega^{n+1} = \Omega^n + F(u^*, \Delta t; \Omega^\theta) + G(v^*, \Delta t; \Omega^\lambda) \tag{3.6}$$

where

$$()^\theta = ()^n + \frac{1}{2} g\,[\overline{v^*}^\theta, \Delta t; ()^n], \text{ and } ()^\lambda = ()^n + \frac{1}{2} f\,[\overline{u^*}^\lambda, \Delta t; ()^n]$$

It is stressed here that we will not actually update Ω^n to Ω^{n+1}. Instead, only the absolute vorticity fluxes will be used for the discretization of the r.h.s of Eq. 3.2 and 3.3. To complete the discretization of (3.2) and (3.3), the pressure gradient terms are discretized with the explicit "forward-backward scheme" (Mesinger and Arakawa 1976), which is stable and second order accurate if it is combined with a *forward-in-time* advection scheme such as the one used here. The final form of the momentum equations are

$$u^{n+1} = u^n + \Delta t \left\{ Y\left(v^*, \Delta t; \Omega^{\lambda}\right) - \frac{1}{A\Delta\lambda \cos\theta}\,\delta_\lambda \left[\kappa^* + \overline{\overline{\Phi^{n+1}}^{\lambda}}^{\theta} \right] \right\} \quad (3.7)$$

$$v^{n+1} = v^n - \Delta t \left\{ X\left(u^*, \Delta t; \Omega^{\theta}\right) + \frac{1}{A\Delta\theta}\,\delta_\theta \left[\kappa^* + \overline{\overline{\Phi^{n+1}}^{\lambda}}^{\theta} \right] \right\}, \quad (3.8)$$

where κ, the upstream-biased "kinetic energy" defined at the four corners of the cell (the hollow circles in Fig. 1), is formulated as

$$\kappa^* = \frac{1}{2}\left\{ X\left(\overline{u^*}^{\theta}, \Delta t; u^n\right) + Y\left(\overline{v^*}^{\lambda}, \Delta t; v^n\right) \right\} \quad (3.9)$$

The above form of κ minimizes the inconsistency in the momentum equation and thus avoided the "Hollingsworth-Kållberg instability". It is noted that (3.6) can be recovered by taking "curl" of the two components, (3.7) and (3.8), of the vector momentum equation. The time-centered winds $\mathbf{V}^* = (u^*, v^*)$ on the C grid are computed by advancing the advective winds at time level n on the C grid (obtained by spatial averaging) for a half time step. For clarity, we describe next the complete cycle of the time marching.

Assuming the time integration starts from time-level n, before updating the prognostic variables on the D grid for a full time step to time-level n+1, the time-centered advective winds (u^*, v^*) on the C grid are computed (cf., 3.7 and 3.8) as follows.

$$h^* = h^n + F\left(u_c^n, \frac{\Delta t}{2}; h^{\theta/2}\right) + G\left(v_c^n, \frac{\Delta t}{2}; h^{\lambda/2}\right) \quad (3.10)$$

$$u^* = u_c^n + \frac{\Delta t}{2}\left\{ Y\left(v^n, \frac{\Delta t}{2}; \Omega_c^{\lambda/2}\right) - \frac{1}{A\Delta\lambda \cos\theta}\,\delta_\lambda\left[\kappa^{**} + \Phi^*\right] \right\}, \quad (3.11)$$

$$v^* = v_c^n - \frac{\Delta t}{2}\left\{ X\left(u^n, \frac{\Delta t}{2}; \Omega_c^{\theta/2}\right) + \frac{1}{A\Delta\theta}\,\delta_\theta\left[\kappa^{**} + \Phi^*\right] \right\}, \quad (3.12)$$

where

$$h^{\lambda/2} = h^n + \frac{1}{2} f\left(u_a^n, \frac{\Delta t}{2}; h^n\right), \quad h^{\theta/2} = h^n + \frac{1}{2} g\left(v_a^n, \frac{\Delta t}{2}; h^n\right),$$

$$\Omega_c^{\lambda/2} = \Omega_c^n + \frac{1}{2} f\left(u_b^n, \frac{\Delta t}{2}; \Omega_c^n\right), \quad \Omega_c^{\theta/2} = \Omega_c^n + \frac{1}{2} g\left(v_b^n, \frac{\Delta t}{2}; \Omega_c^n\right),$$

$$u_b^n = \overline{u^n}^{\lambda}, \quad v_b^n = \overline{v^n}^{\theta},$$

$$u_c^n = \overline{u_b^n}^{\theta}, \quad v_c^n = \overline{v_b^n}^{\lambda},$$

$$u_a^n = \overline{u_c^n}^{\lambda}, \quad v_a^n = \overline{v_c^n}^{\theta},$$

$$\Omega_c^n = 2\omega \sin\theta + \nabla \times \mathbf{V}_c^n,$$

and κ^{**}, the upwind-biased kinetic energy defined at the mass point, is computed as

$$\kappa^{**} = \frac{1}{2}\left[X\left(u_a^n, \frac{\Delta t}{2}; u_c^n\right) + Y\left(v_a^n, \frac{\Delta t}{2}; v_c^n\right) \right] \quad (3.13)$$

After (u^*, v^*) are obtained, prognostic variables h^n and (u^n, v^n) are updated using Eq. 3.5, 3.7, and 3.8.

It is noted that the "divergence" of the advective winds (u^*, v^*) and the "curl" of the prognostic winds (u^n, v^n), the relative vorticity, as well as the "mass" are defined at the same point. Therefore, as far as linear behavior of the system is concerned, this two-grid (C and D) system is essentially the same as Randall's Z grid. Due to the use of the two-step procedure, there is no need to invert the vorticity and divergence, which is a great computational advantage. This two-grid system can therefore be appropriately called the "inverse Z grid".

4. Simulation of a Typhoon-like vortex with the triply nested unified model

The algorithm developed in the previous section is local. Therefore, it can be easily applied to a limited area model if appropriate boundary conditions are supplied. To construct a global model, one simply extends the domain to the whole globe and uses the periodic boundary conditions in the longitudinal direction. The "boundary conditions" at the north and the south poles are more complicated. Relative vorticity at the poles is computed by the Stokes theorem (see LR-b for details). Fluxes into and out of the polar caps are computed the same way as described in Lin et al. (1994). For efficiency reason, a polar Fourier filter can be used in the global model to stabilize high frequency gravity waves that are being unidirectionally resolved at high latitudes.

There are several feasible ways of nesting a fine grid (a limited area model) to a coarser grid, which may or may not be global in extent. To conserve mass in the global grid when there is two-way interaction, one would need to use, instead of the values of the prognostic variables, fluxes (computed in the coarse grid) orthogonal to the boundaries of the fine grid as the boundary conditions. Using fluxes for the specification of the boundary conditions is made possible by the flux-form nature of our algorithm. However, this procedure is difficult to implement if only one model code is to be maintained and used as a global model, a regional model, or a nested global-regional model. For this practical reason, we chose instead to use linear interpolation to obtain the necessary values near the boundaries of the fine grid from the values computed in the coarse grid. If two-way interactions are desired, results from the fine grid are appropriately averaged (to the coarse grid resolution) to replace those coarse grid values in the overlap region. In the unified model code, all the necessary boundary conditions are obtained by calling a single subroutine that performs the linear interpolation (from a coarse grid to a fine grid). Another subroutine performs the averaging process (from a fine grid to a coarse grid). The core of the unified model code can therefore be used for all types of grid.

The unified model has been extensively tested using various initial conditions with or without bottom topography, in the "global mode" or in the stand alone "local mode". To verify the nesting capability of the model, several cases proposed by Williamson et al. (1992) were tested using a triply nested unified model. For brevity, these tests will not be shown here. To demonstrate the utility of the unified model approach, we present here the simulation of the propagation of a Typhoon-like vortex with the fully interactive triply nested unified model. Three grids with increasing resolution (indicated as $\Delta\lambda \times \Delta\theta$ in degrees) were used, which are the global grid ($1.25^o \times 1^o$), the coarse local grid ($0.625^o \times 0.5^o$), and the fine local grid ($0.3125^o \times 0.25^o$). The time step is 900, 450, and 225 seconds, respectively. The computational domains of the two local grids are shown in Fig. 2. The initial condition is a Rankine combined vortex centered at 130E and 15N (the black "dot" east of the Philippines; see Fig. 2) with a 100 km radius and a maximum tangential wind of 50m/s. Since there is no background mean flow or explicit damping mechanism, the vortex maintains a stable circular structure to DAY-14. The direction of the propagation is approximately north-west. Fig. 3 shows the height fields at DAY-5 and DAY-10 in the three grids (only a portion of the global grid is shown). The center of the vortex is over the northern tip of Taiwan at DAY-5, and at DAY-10 the center has propagated to the western boundary of the fine local grid. There is no noises or any peculiar behavior generated by the nesting procedure, which should be attributed to the use of the monotonicity-preserving upstream-biased FFSL scheme.

5. Concluding remarks and future works

We are currently studying the dynamical mechanisms involved in the merger, split, and counter rotating phenomenon (the so-called "Fujiwhara effect") of tropical cyclones using the triply nested unified shallow water model. More detailed cyclone track studies are also planned.

The algorithm described in this paper for the discretization of the shallow water equations can be easily extended to 3-D hydrostatic primitive equations. A working "dynamical core" for the Goddard Earth Observing System General Circulation Model (GEOS-GCM) using a hybrid σ-P vertical coordinate system has already been developed and currently under testing. Finally, it should also be noted that the algorithm described here is self advancing (i.e., no information from the previous time step is needed). Therefore, the core memory usage is, at most, half of that required by the two-time-level semi-Lagrangian models or Eulerian models based on the leap-frog time differencing scheme. The saving in memory can be used, for example, to increase the domain width of the regional model. Combined with the proven higher accuracy of the FFSL scheme, significant improvement over conventional models can be expected.

References:

Arakawa, A., 1966: Computational design for long-term numerical integration of the equations of fluid motions: Two-dimensional incompressible flow. Part I. *J. Comput. Phys.*, **1**, 119-143.

Arakawa, A., and V. R. Lamb, 1981: A potential enstrophy and energy conserving scheme for the shallow water equations. *Mon. Wea. Rev.*, **109**, 18-36.

Bourke, W., 1972: An efficient, one-level, primitive equation spectral model. *Mon. Wea. Rev.*, **100**, 683-689.

Colella, P., and P. R. Woodward, 1984: The piecewise parabolic method (PPM) for gas-dynamical simulations. *J. Comput. Phys.*, **54**, 174-201.

Hollingsworth, A., P. Kållberg, V. Renner, and D. M. Burridge, 1983: An internal symmetric computational instability. *Quart. J. R. Met. Soc.*, **109**, 417-428.

Lin, S.-J., W. C. Chao, Y. C. Sud, and G. K. Walker, 1994: A class of the van Leer-type transport schemes and its applications to the moisture transport in a general circulation model. *Mon. Wea. Rev.*, **122**, 1575-1593.

———, and R. B. Rood, 1995a: Multidimensional flux-form semi-Lagrangian schemes. (submitted to *Mon. Wea. Rev.*)

———, and R. B. Rood, 1995b: An explict flux-form semi-Lagrangian shallow water model on the sphere. (To be submitted to *Quart. J. Roy. Met. Soc.*)

Mesinger, F., and A. Arakawa, 1976: Numerical methods used in atmospheric models. *GARP Publications Series No. 17*, WMO-ICSU Joint Organizing Committee, 64pp.

Randall, D. A., 1994: Geostrophic adjustment and the finite-difference shallow-water equations. *Mon. Wea. Rev.*, **122**, 1371-1377.

Sadourny, R., 1975: The dynamics of finite difference methods of the shallow water equations. *J. Atmos. Sci.*, **32**, 680-689.

Smolarkiewicz, P. K., 1982: The multi-dimensional Crowley advection scheme. *Mon. Wea. Rev.*, **110**, 1968-1983.

Staniforth, A., and J. Côté, 1991: Semi-Lagrangian integration schemes for atmospheric models -- A review. *Mon. Wea. Rev.*, **119**, 2206-2223.

Williamson, D. L., J. B. Drake, J. J. Hack, R. Jakob, and P. N. Swarztrauber, 1992: A standard test set for numerical approximations to the shallow water equations in spherical geometry. *J. Comput. Phys.*, **102**, 211-224.

Woodward, P. R., and P. Colella, 1984: The numerical simulation of two-dimensional fluid flow with strong shocks. *J. Comp. Phys.*, **54**, 115-173.

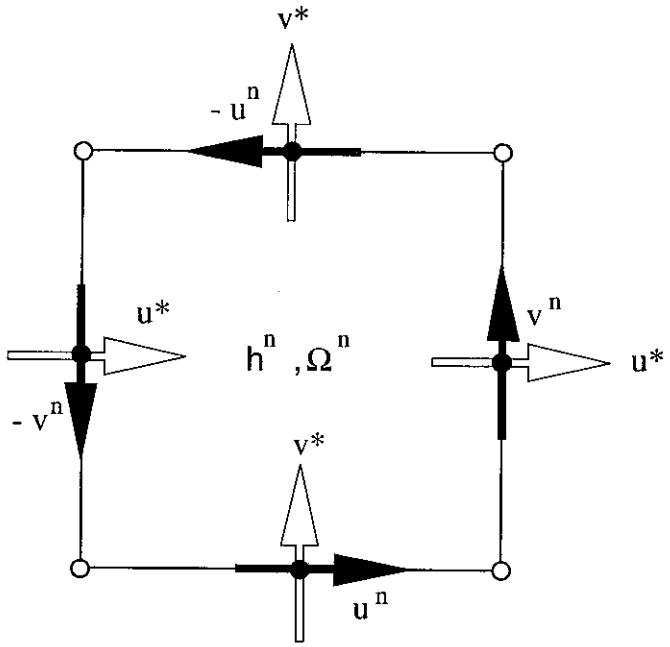

Fig. 1 Schematics of the "inverse Z grid". The time-centered advective winds (the hollow arrows) are staggered as in the C grid whereas the prognostic winds (the solid arrows) are staggered as in the D grid.

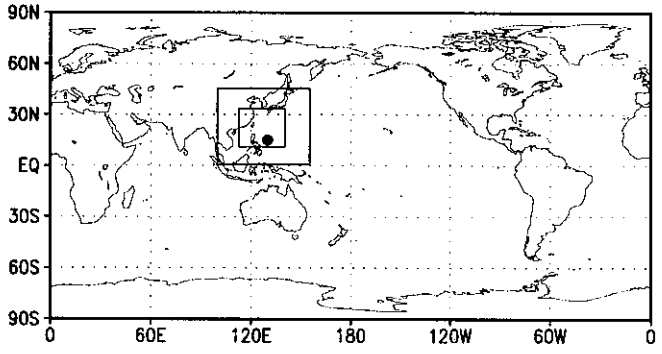

Fig. 2 The triply nested grids. The "black dot" is the initial height contours (contour interval=25 m). The meridional resolutions for the global grid, the coarse local grid, and the fine local grid are approximately 111 km, 55.6 km, and 27.8 km, respectively.

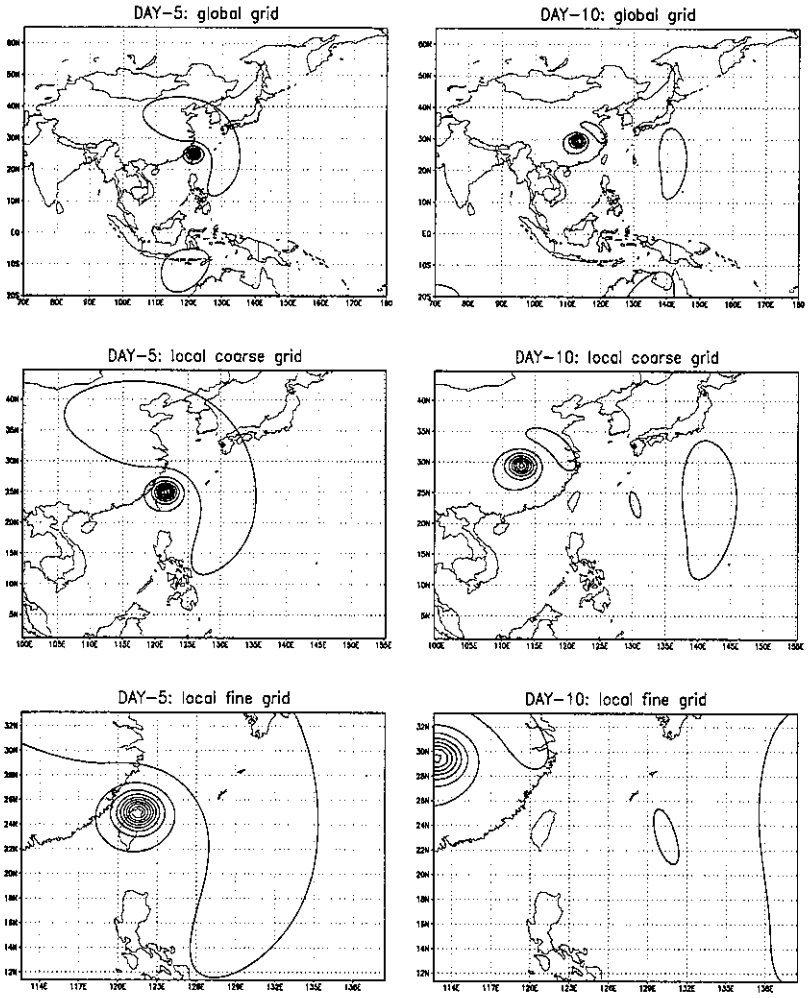

Fig. 3 Height field contours at DAY-5 (contour interval=20m) and DAY-10 (contour interval=15m)